

RESEARCH ARTICLE

p38 MAPK as an essential regulator of dorsal-ventral axis specification and skeletogenesis during sea urchin development: a re-evaluation

Maria Dolores Molina, Magali Quirin, Emmanuel Haillet, Felipe Jimenez, Aline Chessel and Thierry Lepage*

ABSTRACT

Dorsal-ventral axis formation in the sea urchin embryo relies on the asymmetrical expression of the TGF β Nodal. The p38-MAPK pathway has been proposed to be essential for dorsal-ventral axis formation by acting upstream of *nodal* expression. Here, we report that, in contrast to previous studies that used pharmacological inhibitors of p38, manipulating the activity of p38 by genetic means has no obvious impact on morphogenesis. Instead, we discovered that p38 inhibitors strongly disrupt specification of all germ layers by blocking signalling from the Nodal receptor and by interfering with the ERK pathway. Strikingly, while expression of a mutant p38 that is resistant to SB203580 did not rescue dorsal-ventral axis formation or skeletogenesis in embryos treated with this inhibitor, expression of mutant Nodal receptors that are resistant to SB203580 fully restored *nodal* expression in SB203580-treated embryos. Taken together, these results establish that p38 activity is not required for dorsal-ventral axis formation through *nodal* expression nor for skeletogenesis. Our results prompt a re-evaluation of the conclusions of several recent studies that linked p38 activity to dorsal-ventral axis formation and to patterning of the skeleton.

KEY WORDS: Nodal, Sea urchin development, TGF β , p38, ERK, SB203580

INTRODUCTION

In the sea urchin, the dorsal-ventral axis is specified after fertilization by the asymmetrical expression of the TGF β superfamily member Nodal. *nodal* expression is initiated around the 32-cell stage and is rapidly restricted to an ectodermal domain of the early blastula (Molina et al., 2013). This regionalized expression is the earliest known zygotic molecular asymmetry associated with specification of the dorsal-ventral axis. Understanding how *nodal* expression is regulated is therefore essential to understand how the dorsal-ventral axis is specified.

The p38-MAPK pathway has been proposed to be essential for the initiation of *nodal* expression. Embryos treated with the pharmacological inhibitor of p38, SB203580, lacked expression of *nodal* and of its downstream target genes in the ventral ectoderm (Bradham and McClay, 2006). Apparently, SB203580 did not prevent the induction of Nodal target genes in *nodal*-overexpressing embryos, suggesting that p38 functions upstream of *nodal*

expression. Using a phospho-specific anti-p38 antibody and a p38-GFP fusion construct, Bradham and McClay reported that p38 is uniformly activated in all cells during cleavage and is transiently downregulated in presumptive dorsal blastomeres at blastula stage. Surprisingly, however, 10 years after the finding that inhibition of p38 suppresses *nodal* expression, and despite continued efforts by several laboratories, including our own, to identify the transcription factors that control *nodal* expression, the transcription factors regulated by p38 that drive *nodal* expression have remained elusive (Nam et al., 2007; Range et al., 2007; Range and Lepage, 2011).

Recently, an early expressed homeobox gene named *hbox12*, a paralogous member of a family of skeletogenic regulatory genes that includes *pmar1* and *micro1* (Kitamura et al., 2002; Nishimura et al., 2004), has been proposed to act *upstream* of p38 as a negative spatial modulator of the activity of this kinase and as a repressor of *nodal* expression (Cavalieri and Spinelli, 2014). However, there is presently a controversy regarding the expression pattern of this homeobox gene, as well as its proposed activity as a regulator of *nodal* expression (Haillet et al., 2015). Using the same cDNA as the original *hbox12* gene, Haillet et al. failed to reproduce by *in situ* hybridization the lateral expression pattern of *hbox12* and found instead expression of this gene in the skeletogenic precursors (Haillet et al., 2015). In addition, overexpression of the mRNA encoding the original *hbox12* sequence did not affect dorsal-ventral axis formation but caused instead a massive epithelial-mesenchymal transition (EMT), i.e. the prototypical phenotype previously described for members of the *pmar1* and *micro1* families. Furthermore, no link between the activity of the maternal determinant Panda and the expression of this homeobox gene has been found, leaving the issue of the spatial regulation of *hbox12* expression and of p38 activity unresolved (Haillet et al., 2015).

In this study, we revisited the role of p38 in the dorsal-ventral axis and in the regulation of *nodal* expression using a combination of functional and biochemical experiments. We arrived at the unexpected conclusion that p38 function is not required for dorsal-ventral axis formation or for skeletogenesis, and that the effects of pharmacological inhibition of p38 on dorsal-ventral axis formation are largely due to non-specific inhibition of the Nodal receptors by these inhibitors. Therefore, this study prompts a reconsideration of the role of p38 upstream of *nodal* expression and a re-evaluation of the results of recent studies linking the spatial regulation of p38 activation to transcriptional repressors of the Hbox12/Pmar1/Micro1 family and to *nodal* expression.


RESULTS

Genetic activation or inhibition of the p38 pathway fails to perturb dorsal-ventral axis formation and *nodal* expression

Evidence that p38 is required for dorsal-ventral axis formation and for skeletogenesis relies predominantly on the finding that

Université Côte d'Azur, CNRS, INSERM IBV, 06108 Nice cedex 2, France.

*Author for correspondence (tlepage@unice.fr)

 M.D.M., 0000-0001-9353-7920; M.Q., 0000-0001-7967-5622; E.H., 0000-0001-5210-6112; F.J., 0000-0003-2064-6733; T.L., 0000-0003-2889-5064

Received 21 March 2017; Accepted 8 May 2017

Lytechinus variegatus embryos treated with the pyridinyl-imidazole inhibitor of p38 SB203580 at 20 μ M lack a dorsal-ventral axis, fail to express *nodal* and lack a skeleton. Using the Mediterranean sea urchin *Paracentrotus lividus*, we confirmed that treatments with SB203580 at 20 μ M also disrupt skeletogenesis and abrogate establishment of the dorsal-ventral axis due to absence of *nodal* expression (Figs 1 and 2). In addition, embryos treated with SB203580 fail to form mesenchymal precursors of the skeleton and gastrulate abnormally, with either no archenteron being formed or,

on the contrary, several small invaginations being present at late gastrula stage (asterisks in Fig. 1A). In fact, most embryos treated with SB203580 develop into balls of cells; they do not swim and lie on the bottom of the Petri dish where they do not seem to differentiate further. The phenotype caused by treatment with SB203580 at 20 μ M is therefore highly pleiotropic, apparently disrupting specification of all germ layers and affecting morphogenesis in multiple ways. Unexpectedly, neither activation of p38 by overexpression of an activated version of the upstream

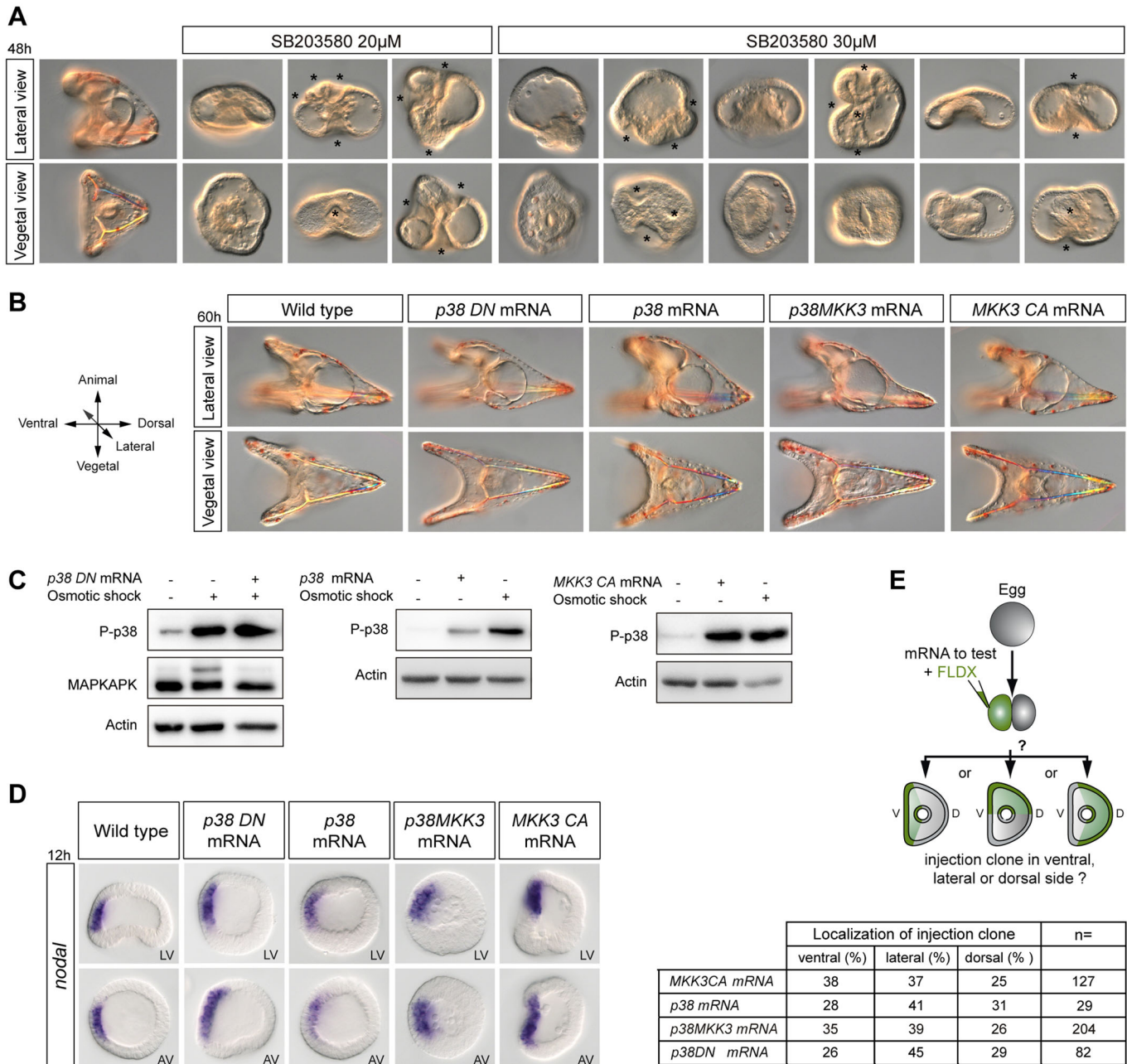


Fig. 1. Genetic perturbations of the p38 pathway do not affect dorsal-ventral axis formation or *nodal* expression. (A) Range of phenotypes caused by high concentrations of SB203580. Multiple invaginations of the epithelium are indicated by asterisks. (B) Normal morphogenesis of embryos following overactivation or inhibition of p38 signalling. (C) Western blot assay to test for p38 activation and p38 activity at hatching blastula stage. Densitometric analysis using ImageJ indicated that embryos treated with the hyperosmotic buffer show a 300% increase in phospho-MAPKAPK levels. In contrast, embryos overexpressing the dominant-negative p38 and treated with the high-salt buffer show a basal level of phospho-MAPKAPK equivalent to that in control untreated embryos. (D) *nodal* expression following genetic perturbations of p38 signalling. LV, lateral view; AV, animal pole view. (E) Axis orientation assays to test the ability of the constructs to define the dorsal-ventral axis. V, ventral; D, dorsal.

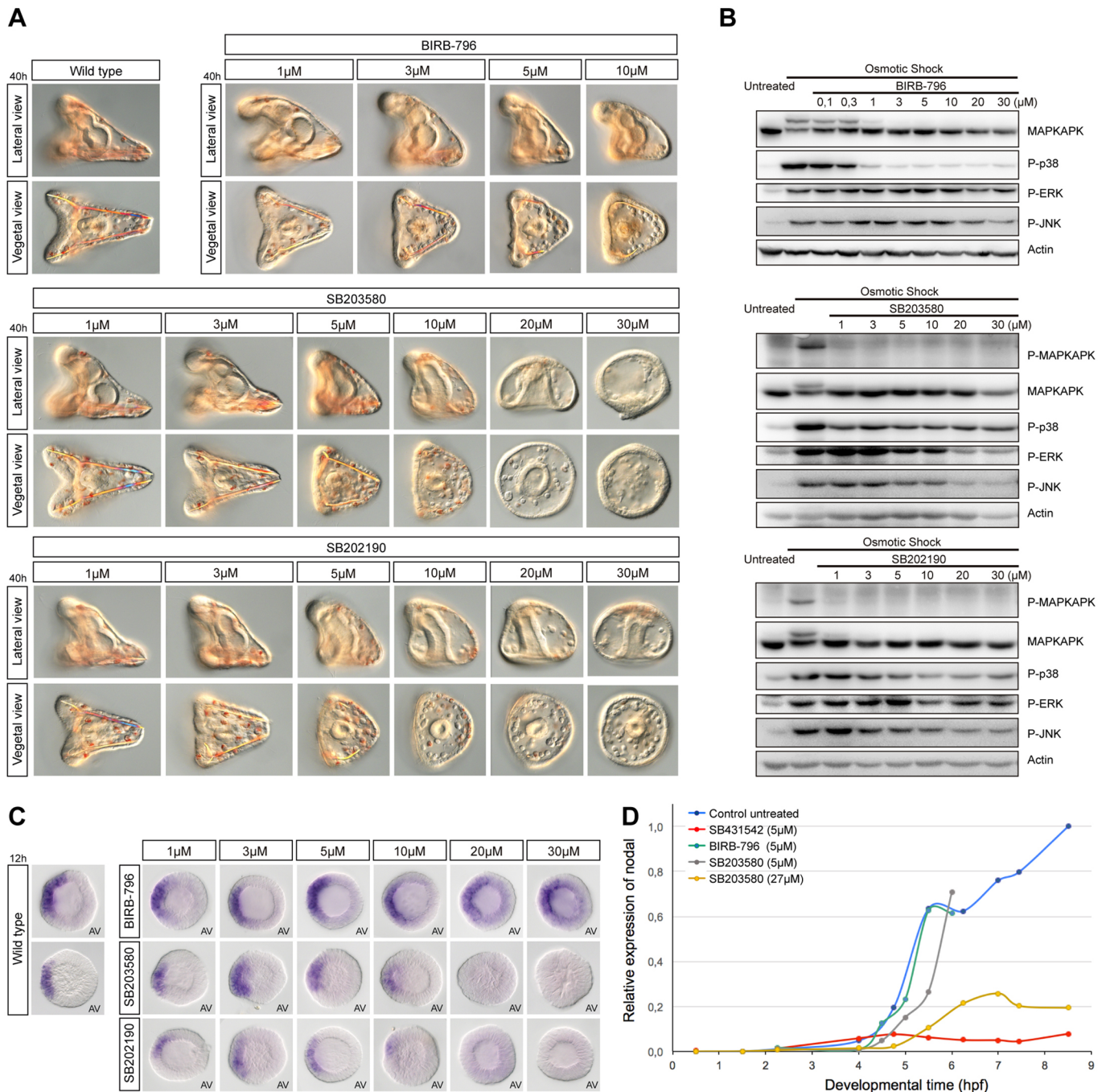


Fig. 2. High concentrations of SB203580 and SB202190, but not BIRB-796, suppress *nodal* expression and disrupt MAPK signalling. (A) Phenotypes caused by inhibitors of p38 at increasing concentrations. (B) Western blot analysis at hatching blastula stage of control and embryos treated with the inhibitors for 1 h. The activity of p38 measured by its ability to phosphorylate MAPKAPK after an osmotic shock is suppressed in the presence of inhibitors starting at concentrations of 1 μ M. (C) *nodal* expression analysed by *in situ* hybridization. AV, animal pole view. (D) QPCR analysis of *nodal* expression. hpf, hours post-fertilization at 22°C. *nodal* expression is initiated normally in embryos treated with BIRB and SB203580 at 5 μ M, a concentration five times higher than that required to inhibit p38.

kinase MKK3 (MKK3-CA) or by creating a fusion between p38 and MKK3, nor inhibition of p38 by overexpression of a dominant-negative (kinase dead) version of p38, interfered with dorsal-ventral axis formation and all injected embryos developed into perfectly normal pluteus larvae (Fig. 1B). The observation that overexpression of the dominant-negative p38 did not block dorsal-ventral axis formation was particularly surprising as Bradham and McClay had observed dorsal-ventral defects caused by overexpression of a

catalytically inactive non-phosphorylatable dominant-negative p38 construct (Bradham and McClay, 2006).

To control p38 activation in embryos injected with these constructs, we designed an assay based on activation of p38 signalling induced by osmotic stress, a well-characterized activator of p38 (Han et al., 1994; Raingeaud et al., 1995; Rouse et al., 1994) (Fig. 1C). Briefly, embryos were placed in conditions of hyperosmolarity and p38 activation was monitored by western blot using

a p38 phospho- (Thr180-Tyr182) antibody (Fig. 1C). In addition, to monitor p38 activity, we measured the level of phosphorylation of MAPKAPK, a direct target and an emblematic substrate of p38 (Cuadrado and Nebreda, 2010; Lee et al., 1994) (see Fig. S1). The level of phospho-MAPKAPK was low in control untreated embryos. As expected, the osmotic stress efficiently activated p38 and triggered rapid phosphorylation of MAPKAPK, causing a shift in its electrophoretic mobility that could be detected by western blot using the antibody against the non-phosphorylated form of human MAPKAPK. This effect was largely blocked by the dominant-negative p38 (Fig. 1C). However, overexpression of wild-type p38 or of MKK3-CA caused a striking increase in the level of phosphorylation of p38 similar to that caused by the osmotic shock. These results show that our p38 constructs are functional.

We then analysed *nodal* expression by *in situ* hybridization in embryos injected with these mRNAs (Fig. 1D). In agreement with the normal morphology of larvae injected with these constructs, neither the activation of p38 signalling by overexpression of wild-type p38, MKK3-CA or p38-MKK3, nor inhibition of p38 signalling achieved by overexpression of a dominant-negative p38 perturbed *nodal* expression (Fig. 1D, Fig. S2).

Finally, to further evaluate the role of the p38 pathway in secondary axis formation, we used a different assay based on the ability of locally overexpressed genes to orient the dorsal-ventral axis (Haillet et al., 2015). mRNAs encoding components that activate or that inhibit the p38 pathway were injected into one blastomere at the two-cell stage together with a lineage tracer, and the position of the tracer in regard of the dorsal-ventral axis was scored at gastrula stage (Fig. 1E). None of the components of the p38 pathway tested influenced significantly the orientation of the secondary axis. Altogether, these results do not support the idea that p38 signalling is crucially required for establishment of the dorsal-ventral axis. They suggest instead that the effects of SB203580 on dorsal-ventral axis formation are unrelated to inhibition of p38-MAPK activity.

Pharmacological inhibition of the p38 pathway has no effect on dorsal-ventral axis formation

Because genetic suppression of the p38 pathway did not affect dorsal-ventral axis formation and *nodal* expression, we re-evaluated the effects of pharmacological inhibitors of p38 on early development of the sea urchin. We tested the effects on dorsal-ventral axis formation of three different p38 inhibitors belonging to two different families. SB203580 and SB202190 belong to the pyridinyl-imidazole class of p38 inhibitors. These compounds act by binding to the ATP-binding pocket of p38, blocking its activity. BIRB-796 is also a potent inhibitor of p38, which belongs to the urea-diaryl family and has been demonstrated to be more specific than pyridinyl-imidazole inhibitors of p38 (Bain et al., 2007). BIRB-796 blocks p38 activity by a mechanism that is different from that used by SB203580 and SB202190, and involves a conformational change that locks the kinase in an inactive form (Kuma et al., 2005; Pargellis et al., 2002).

All three inhibitors efficiently blocked p38 activity when used at concentrations as low as 1 μ M, consistent with the concentrations usually recommended for the use of these chemicals (Fig. 2B) (Bain et al., 2007). Remarkably, for all three chemicals, embryos treated with concentrations of inhibitors that were sufficient to inhibit p38 activity developed into perfectly normal pluteus larvae (Fig. 2A). Embryos treated with BIRB-796 at doses up to ten times higher (10 μ M) developed largely normally with a clearly defined dorsal-ventral axis, but displayed signs of toxicity late in gastrulation.

When used at 5 μ M, both SB202190 and SB203580 slightly perturbed morphogenesis but embryos developed with a well-recognizable dorsal-ventral axis and a correctly patterned skeleton. Only when much higher concentrations (10 μ M and above) of SB202190 or SB203580 were used were inhibition of dorsal-ventral axis formation and severe skeletogenesis defects observed. As described above in the case of SB203580, at these high doses, the two pyridinyl-imidazole inhibitors blocked ingression of the primary mesenchymal cells (PMCs) (Fig. S3), variably blocked invagination of the archenteron and inhibited motility, which resulted in poorly patterned larvae with no mesoderm, no skeleton and no dorsal-ventral axis. The fact that these severe and pleiotropic defects were only observed at doses twenty to thirty times more elevated than the doses sufficient to block p38 activity raised the possibility that these phenotypes could be unrelated to inhibition of p38 activity, but could result instead from non-specific inhibition of other kinases. Indeed, western blot analysis of phospho-ERK and phospho-JNK revealed that, in addition to blocking p38 activity, high doses of SB203580, but not of BIRB-796, potently inhibited activation of ERK and JNK following an osmotic shock. This strongly suggests that SB203580 and SB202190 may interfere with other MAP kinase pathways when used at high concentration (Fig. 2B). As ingression and differentiation of the PMCs (precursors of the skeleton), and skeletogenesis in general, crucially require a functional Raf/MEK/ERK pathway (Fernandez-Serra et al., 2004; Rottinger et al., 2004), the finding that SB203580 severely blocked the activation of this pathway by the osmotic stress raised the possibility that the same drug might also inhibit the Raf/MEK/ERK pathway during normal development.

Only high concentrations of pyridinyl-imidazole inhibitors, but not of the more specific p38 inhibitor BIRB-796, abolish *nodal* expression

To further characterize the effects of p38 inhibitors on dorsal-ventral axis formation, we analysed *nodal* expression by QPCR and *in situ* hybridization in embryos treated continuously with either pyridinyl-imidazole inhibitors or with BIRB-796 at various concentrations from fertilization onwards. *In situ* hybridization revealed that *nodal* expression was largely normal in embryos treated with SB203580, SB202190 or BIRB-796 at concentrations up to 10 μ M (Fig. 2C), consistent with the presence of a well-established dorsal-ventral axis in these embryos (Fig. 2A). Only when SB203580 or SB202190 were used at a concentration close or equal to 20 μ M was expression of *nodal* strongly reduced or abolished (Fig. 2C). In contrast, *nodal* expression was unaffected in embryos treated with the more-specific p38 inhibitor BIRB-796 at the most elevated concentration (30 μ M). QPCR analysis confirmed that *nodal* expression was initiated normally in embryos treated with doses five times higher than the dose required to inhibit p38 and that only doses of SB203580 that were 30 times above the dose required to block p38 significantly affected *nodal* expression (Fig. 2D). These results suggest that the failure of *nodal* expression caused by SB203580 and SB202190, when used at high doses, is not due to inhibition of p38 activity but likely results from non-specific inhibition of other targets.

High concentrations of pyridinyl-imidazole inhibitors cause pleiotropic and non-specific effects in the ectoderm, mesoderm and endoderm, in part by blocking the ERK pathway

To understand why SB203580 and SB202190 cause such pleiotropic effects on early sea urchin development, we examined the effects of treatments with these inhibitors on the expression of

molecular marker genes of all three germ layers by *in situ* hybridization. Embryos were treated starting after fertilization with SB203580, SB202190 or BIRB-796 and fixed at swimming blastula stage. Treatments with increasing concentrations of pyridinyl-imidazole inhibitors resulted in a dose-dependent reduction of the expression of *chordin* (Bradham et al., 2009; Lapraz et al., 2009) in the ectoderm as well as in downregulation of the expression of *Delta* (McClay et al., 2000; Sweet et al., 2002) in the skeletogenic mesoderm and *gcm* in the non-skeletogenic mesoderm (Ransick and Davidson, 2006) (Fig. 3A). Consistent with the reduced expression of *Delta* in the mesodermal precursors, immunostaining at blastula stage revealed that the level of ERK activation in precursors of the skeletogenic mesoderm disappeared following treatment with the highest doses of pyridinyl-imidazole inhibitors (Fig. 3B). Unexpectedly, expression of *foxaq2* (Tu et al., 2006; Yaguchi et al., 2006) in the animal pole domain was eliminated, whereas expression of the endodermal marker gene *foxa* (Oliveri et al., 2006) appeared stronger and significantly expanded in embryos treated with SB203580 at 30 μ M (Fig. 3A,C). The expanded expression of *foxa* suggests that the ectopic invaginations of the epithelium observed following treatments with high doses of SB203580 (Fig. 1A) may be ectopic guts similar to the ectopic guts generated by overactivation of the Wnt/ β -catenin pathway (Wikramanayake et al., 1998). In contrast, consistent with the lack of effects of genetic perturbations of p38 pathway components (Fig. S2), all the above-mentioned marker genes were expressed at normal levels in embryos treated with the more specific p38 inhibitor BIRB-796 at doses up to 30 μ M (Fig. 3A,B).

Finally, we tested the effects of p38 inhibitors on ERK activation by western blot. Protein extracts were prepared from embryos treated from fertilization with increasing doses of these inhibitors and the

level of activation of ERK was evaluated by western blot (Fig. 3D). Strikingly, consistent with the results of immunostaining, treatment with pyridinyl-imidazole inhibitors at high concentration, but not with BIRB-796, caused a drastic reduction of phosphorylation of ERK. This demonstrates that, in addition to blocking the p38 pathway, high doses of pyridinyl-imidazole inhibitors non-specifically disrupt activation of the ERK pathway, which plays a central role in skeletogenesis in the sea urchin embryo (Fernandez-Serra et al., 2004; Rottinger et al., 2004). These results, therefore, strongly suggest that the conclusions regarding the role of p38 in skeletogenesis that relied on treatments with these inhibitors at high concentrations (Bradham and McClay, 2006) have to be taken with great caution, as the observed effects are most likely caused, at least in part, by non-specific inhibition of the Raf/MEK/ERK pathway.

Treatment with SB203580 at high concentrations disrupts both initiation and maintenance of *nodal* expression

A previous study in *Lytechinus variegatus* had concluded that p38 is activated at 60-cell stage and that early blastula is the end point of the p38 requirement for oral specification; this led to the conclusion that p38 is required only for initiation and not for maintenance of *nodal* expression (Bradham and McClay, 2006). Consistent with previous reports, we found that a basal level of p38 is already detected at the two-cell stage and that the level of p38 activation increases very slowly during cleavage up to the 8th cleavage, when the level of phospho-p38 increases abruptly (Fig. 4A). As *nodal* expression is initiated around the 32-cell stage, the timing of p38 activation does not match well with the kinetics of *nodal* expression. We also re-analysed the effects of late treatments with p38 inhibitors on *nodal* expression by treating embryos with SB203580 or BIRB-

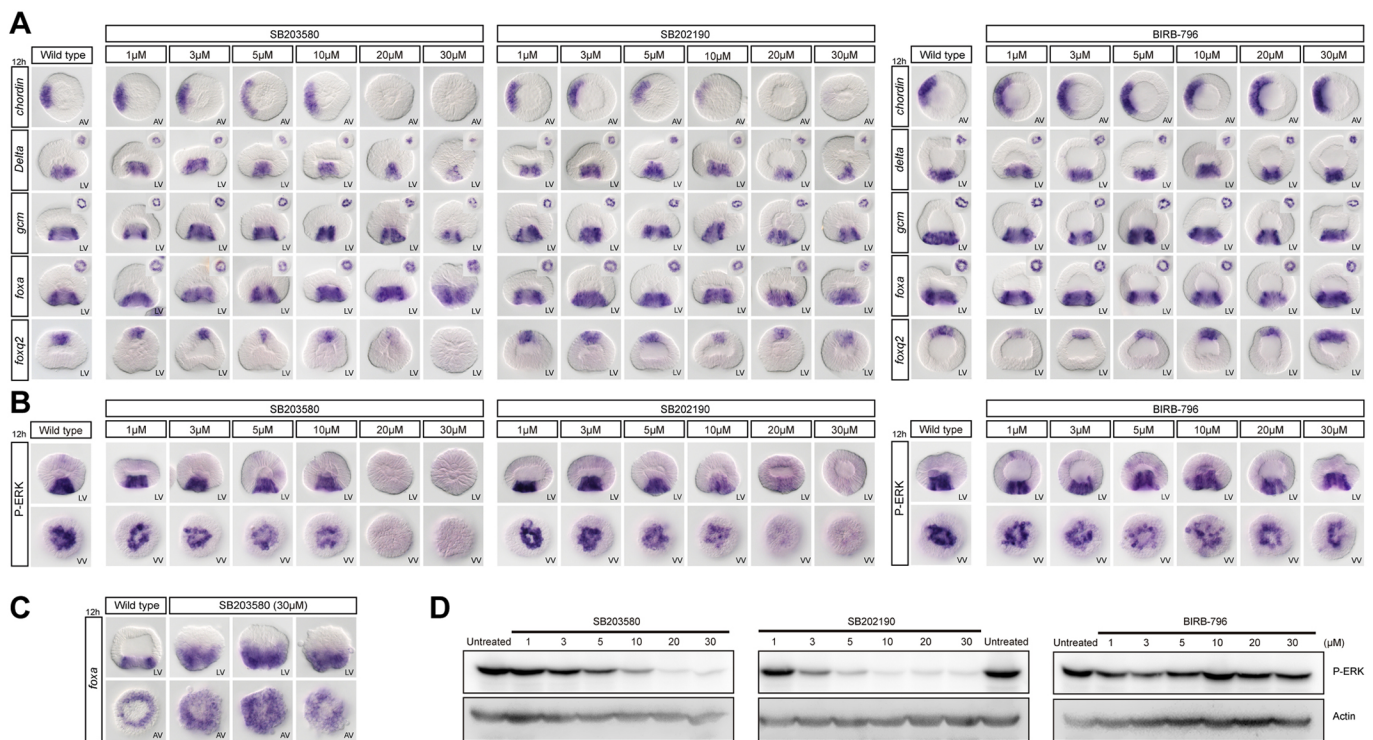


Fig. 3. High concentrations of pyridinyl-imidazole inhibitors, but not of BIRB-796, disrupt specification of all germ layers. (A) Expression of *chordin*, *Delta*, *gcm*, *foxa* and *foxq2* by *in situ* hybridization in embryos treated with increasing concentrations of p38 inhibitors. Vegetal views are shown in the upper corner of some of the images. (B) Phospho-ERK immunostaining. (C) *foxa* *in situ* hybridization after treatment with SB203580 at 30 μ M. Three representative embryos are shown. (D) Western blot analysis of P-ERK activation at hatching blastula stage. LV, lateral view; AV, animal pole view; VV, vegetal pole view.

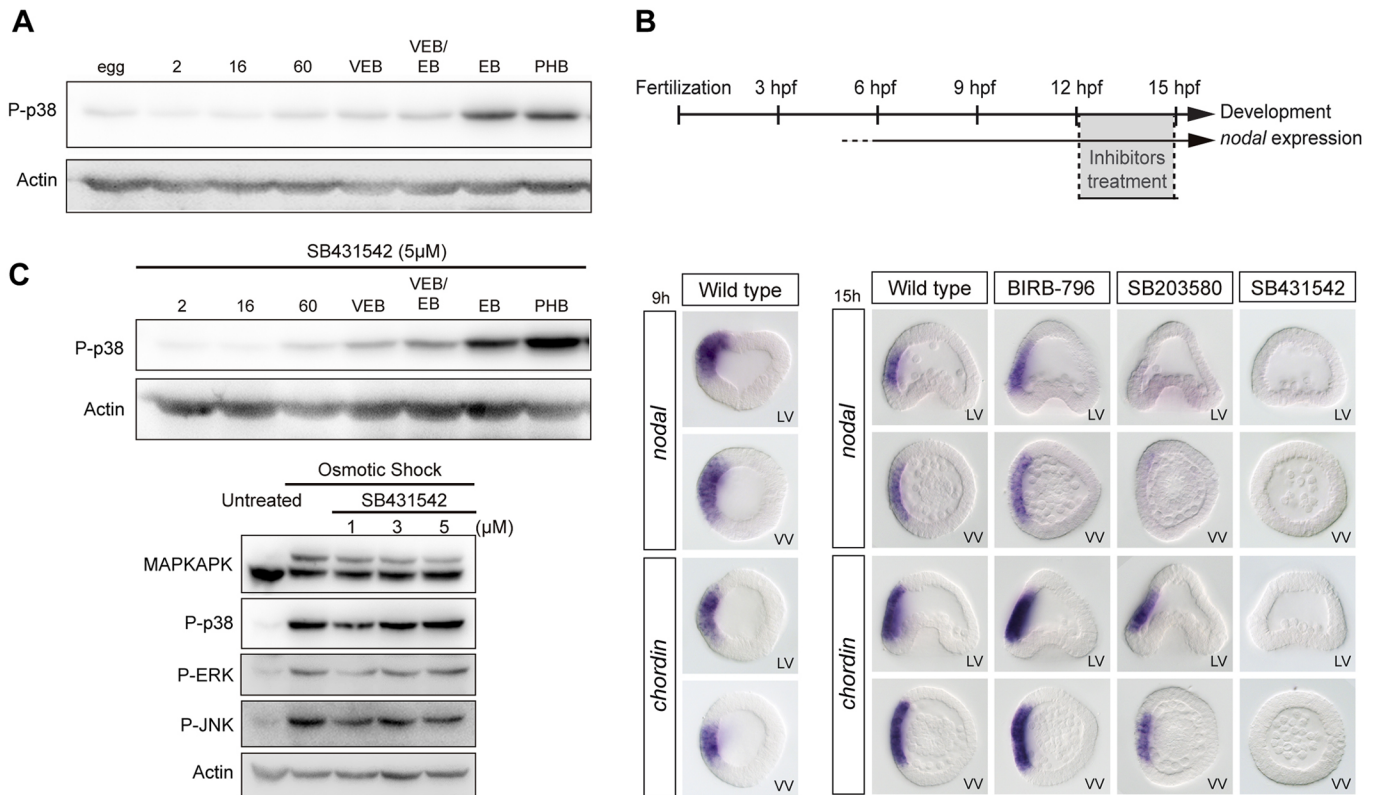


Fig. 4. Pyridinyl-imidazole inhibitors of p38, but not BIRB-796, disrupt the Nodal auto-regulatory loop. (A) Western blot of p38 activation during development. (B) Expression of *nodal* and *chordin* by *in situ* hybridization in controls and in embryos treated with the p38 inhibitors SB203580 (30 μM) or BIRB-796 (30 μM), or the Nodal receptor inhibitor SB431542 (5 μM) at 12 hpf. (C) Western blot of p38 activation during development after inhibition of the Nodal receptor by treatment with SB431542. LV, lateral view; VV, vegetal pole view. In C, 2, 16 and 60 refer to the number of cells; VEB, very early blastula; EB, early blastula; PHB, prehatching blastula.

796 at 30 μM, starting at different time points from the egg-cell stage to early gastrula. When started at late blastula stages, 3 h treatments with the p38 inhibitor SB203580 at 30 μM strongly reduced or abolished *nodal* expression. In contrast, treatments with BIRB-796 at doses up to 30 μM, did not affect *nodal* expression (Fig. 4B). Altogether, these results do not support the idea that p38 is required specifically for initiation of *nodal* expression. They suggest instead that either the p38 inhibitors disrupt the Nodal autoregulatory loop, which is crucial for maintenance of *nodal* expression (Nam et al., 2007; Range et al., 2007), or that p38 is required downstream of Nodal. To test whether p38 is required downstream of signalling from the Nodal receptor, we compared the levels of activation of p38 in control embryos and in embryos treated with the Nodal receptor inhibitor SB431542 (Fig. 4C). p38 activation, like ERK or JNK activation, was largely unaffected by inhibition of Nodal signalling, suggesting that p38 is not activated downstream of this signalling pathway.

SB203580 strongly reduces signalling from the Nodal receptor

The finding that BIRB-796 efficiently blocks p38 activity without reducing *nodal* expression strongly suggested that p38 inhibition is not responsible for the suppression of *nodal* expression caused by SB203580 and SB202190, and raised the possibility that these chemicals could affect other factors/pathways required for *nodal* expression. Indeed, several studies have reported that the pyridinyl-imidazole inhibitors SB203580 and SB202190, in addition to being potent inhibitors of p38, can strongly inhibit signalling from the

TGFβ receptor Alk5, as well as signalling by Activin, with IC₅₀ values of 6 μM or 3 μM, respectively (Eyers et al., 1998; Fu et al., 2003; Inman et al., 2002; Laping et al., 2002). Because Alk5 from vertebrates is highly related to the sea urchin Nodal receptor Alk4/5/7, this raised the possibility that the effects of pyridinyl-imidazoles on *nodal* expression could be caused by non-specific inhibition of Alk4/5/7, due to binding of the drug to the ATP-binding pocket of the Nodal receptor. To test this hypothesis, we evaluated the ability of SB203580 to inhibit the induction of Nodal target genes, such as *nodal* and *chordin*, by treatment with recombinant Nodal proteins (Saudemont et al., 2010) or with nickel chloride, an agent that causes massive ectopic expression of *nodal* (Duboc et al., 2004), as well as the ability of the drug to block the activity of a constitutively active Alk4/5/7 (Lapraz et al., 2009). When added to embryos at swimming blastula stage, recombinant Nodal protein robustly induced ectopic expression of *nodal* in the ectoderm (Fig. 5A). As expected, pre-treatment of embryos with the Nodal receptor inhibitor SB431542 completely blocked the induction of *nodal* expression by exogenous Nodal protein. Strikingly, pre-treatment of the embryos with 30 μM of SB203580 also strongly reduced the induction of *nodal* caused by treatment with Nodal protein, by overexpression of a constitutively active version of Alk4/5/7 or by treatment with nickel (Fig. 5A,B). Taken together, these results strongly suggest that the suppression of *nodal* expression in response to high doses of SB203580 is not caused by inhibition of p38 but most likely results from disruption of the Nodal autoregulatory loop.

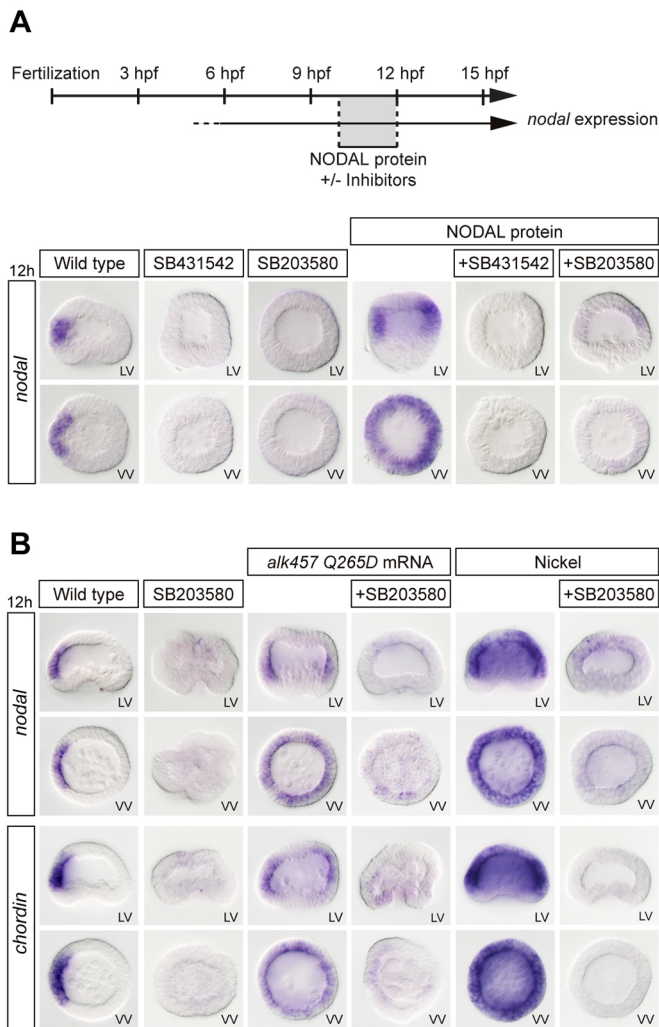


Fig. 5. SB203580 blocks Nodal signalling. (A) *nodal* *in situ* hybridization. SB203580 (30 μ M), like the Nodal receptor inhibitor SB431542 (5 μ M), blocks the ability of exogenous Nodal protein to induce expression of *nodal*. (B) *nodal* and *chordin* *in situ* hybridization. SB203580 blocks the ability of an activated Alk4/5/7 Nodal receptor and of treatments with nickel to induce *nodal* and *chordin* expression. LV, lateral view; VV, vegetal pole view.

Pyridinyl-imidazole-resistant Alk4/5/7 and ACVRII mutants rescue *nodal* expression in the presence of SB203580

Previous studies in vertebrates have shown that a major concern when using pyridinyl-imidazole compounds, such as SB203580 and SB202190, to block p38 activity *in vivo* is that the observed effects of these drugs may result from non-specific inhibition of targets different from p38 (Bain et al., 2007). The reason for the lack of specificity of these inhibitors is that they bind to the ATP-binding pocket of kinases and therefore they may bind to other structurally related but functionally different kinases. Eysers and colleagues have elegantly shown that this problem can be addressed by examining whether the effects of these inhibitors can be suppressed in cells that express an SB203580-resistant mutant form of p38 (Eysers et al., 1998, 1999; Gum et al., 1998; Hall-Jackson et al., 1999; Ho et al., 2006; Wilson et al., 1997). The rationale behind this idea is that it has been established that for a protein kinase to be inhibited by SB203580, the side chain of the residue present at the position equivalent to Thr106 within the ATP-binding pocket of human p38 must not be larger than a threonine. Therefore, replacing this residue with a methionine prevents binding of the drug and renders the

kinase resistant to the inhibitor. Interestingly, the sea urchin VEGF receptor (Duloquin et al., 2007), the type I Nodal receptor Alk4/5/7 (Lapraz et al., 2009) and the type II Nodal receptor ACVRII (Lapraz et al., 2006) have a serine in that position, suggesting that they can potentially all be inhibited by SB203580 (Fig. 6A and Fig. S4). We therefore reasoned that if p38 is specifically required upstream of *nodal* expression, then expression of a mutant p38 resistant to the inhibitor should restore *nodal* expression in embryos treated with SB203580. In contrast, if SB203580 binds non-specifically to the ATP-binding pocket of Alk4/5/7 and ACVRII, thereby inhibiting their activity, then replacing these serine residues with a methionine should make these receptors resistant to SB203580 and should rescue *nodal* expression in sea urchin embryos treated with SB203580. We therefore constructed a mutant p38 (p38-T105M), a mutant Alk4/5/7 (Alk4/5/7-S334M) and a mutant ACVRII (ACVRII-S288M) resistant to SB203580 to perform rescue experiments. We first confirmed by western blot that expression of the mutant p38-T105M but not expression of the mutant Nodal receptor Alk4/5/7-S334M rescued p38 activity in the presence of SB203580 at 30 μ M (Fig. 6B). We then injected mRNA encoding these modified kinases into eggs and let the embryos develop in the presence of either SB431542 or SB203580 at doses that normally completely suppress *nodal* expression (30 μ M). At blastula stage, the embryos were fixed and *nodal* and *chordin* expression was examined by *in situ* hybridization.

Embryos injected with p38-T105M and cultured in the presence of SB203580 developed with exactly the same phenotype as control embryos treated with this inhibitor. They lacked a dorsal-ventral axis and did not express *nodal* and *chordin* at blastula stage (Fig. 6C). Therefore, expression of a mutant p38 that is resistant to SB203580 did not rescue *nodal* expression, unequivocally demonstrating that the disruption of the dorsal-ventral axis caused by SB203580 is not caused by inhibition of p38. Importantly, overexpression of the mutant p38 that is resistant to the inhibitor did not rescue *Delta* expression (Fig. S5) or any of the skeleton defects caused by SB203580, consistent with our finding that, in addition to blocking p38 signalling, this inhibitor disrupts Raf/MEK/ERK signalling. In contrast, although treatment with SB431542 (which also binds to the ATP-binding pocket of Alk4/5/7) eliminated *nodal* expression, most embryos treated with SB431542 but expressing the Alk4/5/7-S334M mutant showed a full rescue of *nodal* expression in the ectoderm and developed with a dorsal-ventral axis (Fig. 6C and Fig. S6). Similarly, although nearly all embryos treated with SB203580 at 30 μ M failed to express *nodal* and *chordin* at blastula stage, embryos expressing either the Alk4/5/7-S334M or the ACVRII-S288M mutations displayed a significant rescue of *nodal* and *chordin* expression in the presence of SB203580. Finally, embryos co-expressing both mutant proteins showed a strong expression of *nodal* both in the presence of SB431542 and SB203580 (Fig. 6C and Fig. S6). These results establish that the phenotypes previously attributed to inhibition of p38, including inhibition of *nodal* expression and disruption of skeletogenesis, are not due to inhibition of p38. The disruption of *nodal* expression is due to the non-specific inhibition of Alk4/5/7 and ACVRII, and the defects associated with skeletogenesis are most likely due to disruption of Raf/MEK/ERK signalling (Fig. 6A).

A transient gradient of p38 activation is generated after initiation of Nodal signalling independently of *hbox12* function

In *Lytechinus*, p38 is activated in all cells at early blastula and transiently inactivated in presumptive dorsal cells, generating a

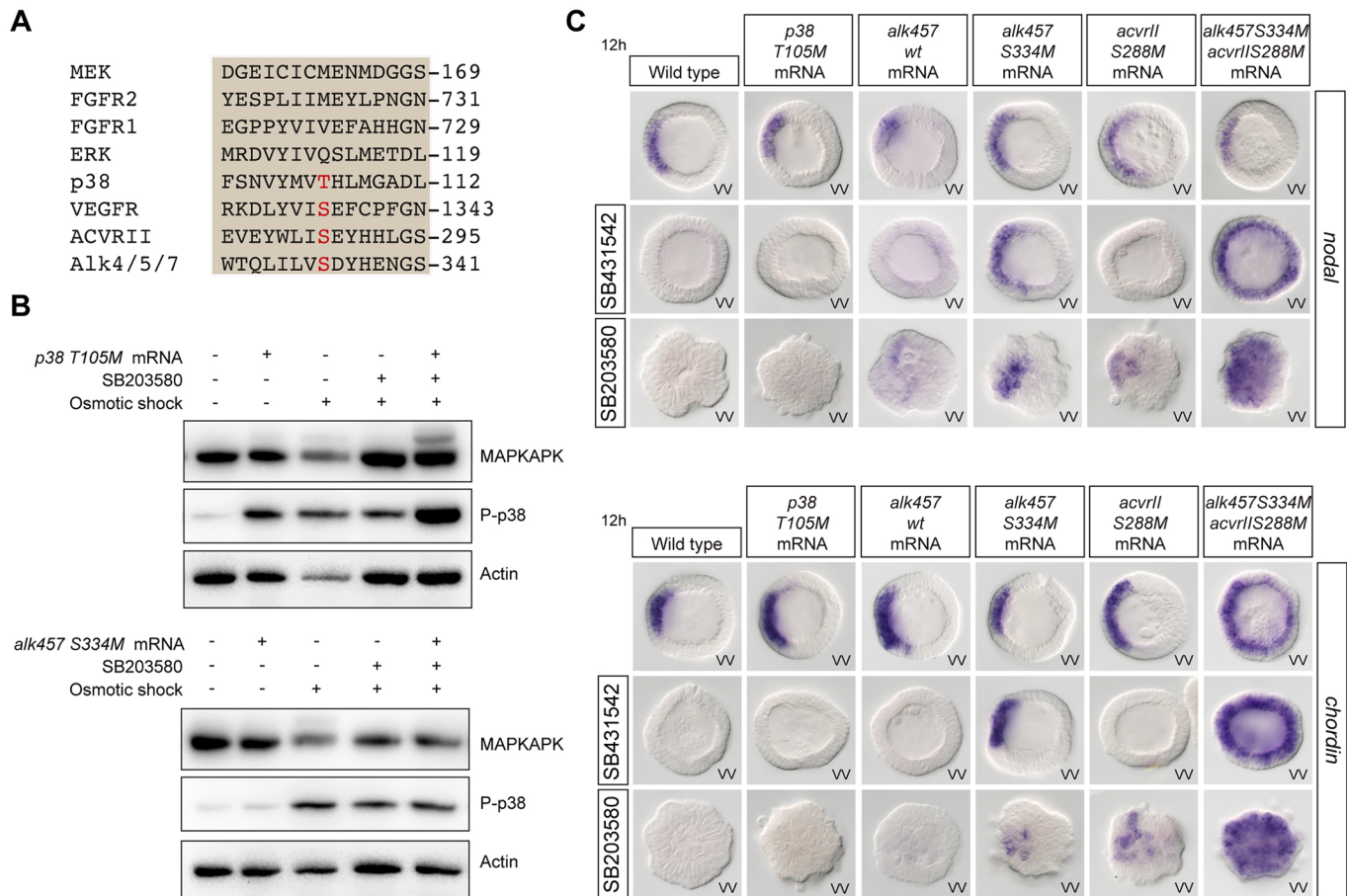


Fig. 6. Inhibitor-resistant Nodal receptors, but not inhibitor-resistant mutant p38, rescue *nodal* expression in the presence of SB203580. (A) Amino acid sequence alignment surrounding Thr105 of p38 in sea urchin MEK, FGFR2, FGFR1, ERK, p38, VEGFR, ACVRII and Alk4/5/7. The presence of Ser or Thr at this gatekeeper position is diagnostic of sensitivity to the inhibitor, whereas the presence of residues with a more bulky lateral chain, such as Met, Gln or Val, is diagnostic of resistance to the inhibitor. (B) Western blot assay at hatching blastula stage. An inhibitor-resistant mutant p38, but not an inhibitor-resistant mutant Alk4/5/7, rescues p38 activity in the presence of SB203580 at 30 μ M. (C) *nodal* and *chordin* *in situ* hybridization. Gatekeeper mutations in ACVRII and Alk4/5/7, but not gatekeeper mutations in p38, rescue *nodal* and *chordin* expression in the presence of SB203580 at 30 μ M. WV, vegetal pole view.

gradient of p38 activation (Bradham and McClay, 2006). This finding was recently confirmed on *Paracentrotus* embryos using a p38-GFP construct (Cavalieri and Spinelli, 2014). Using two different antibodies against the doubly phosphorylated form of p38, we were able to visualize a transient gradient of nuclear p38 in a variable percentage of embryos from the early blastula stage to pre-hatching blastula stage (Fig. 7A). Asymmetric phospho-p38 nuclearization was largely suppressed in embryos ventralized by treatment with Nodal protein (data not shown) or following treatment with nickel (Fig. 7B). However, this gradient was not affected by treatments with the Nodal receptor blocker SB431542 or by overexpression of the maternal determinant of the dorsal-ventral axis *Panda* (Fig. 7B,C), confirming that this gradient may not be established as a direct consequence of Nodal signalling, as it was already suggested (Bradham and McClay, 2006). Moreover, inhibition of p38 did not alter the ability of *panda* mRNA to orient the dorsal-ventral axis (Fig. 7D), further suggesting that establishment of the dorsal-ventral axis is independent of p38 function.

Previous reports, which relied on overexpression of a p38-GFP fusion construct, proposed a role for the transcriptional repressor Hbox12 in the spatial regulation of p38 activation (Cavalieri and Spinelli, 2014). Using a cDNA sequence 100% identical to the published *hbox12* mRNA, we did not find any evidence that Hbox12 overexpression can repress activation of endogenous p38

(Fig. 7C). Instead, overexpression of *hbox12* promoted a massive epithelial-mesenchymal transition, which is exactly the phenotype caused by overexpression of the PMC lineage regulatory genes *pmar1* and *micro1* (Kitamura et al., 2002; Nishimura et al., 2004; Oliveri et al., 2003).

Finally, in an effort to find a function for this gradient of p38 activation, we tested whether graded p38 signalling contributes to the amplitude of the response of cells to Nodal and compared the expression of *nodal* and *lefty*, two Nodal-responsive genes, in control embryos and in embryos treated with BIRB-796. A slight delay of *nodal* and *lefty* expression was detected at 7 h following inhibition of p38 (Fig. 7E). However, at 8 h and later, *lefty* expression in BIRB-796-treated embryos was indistinguishable from that in control embryos.

In conclusion, although a gradient of p38 activation is transiently visible in the early embryo, genetic perturbations, pharmacological inhibition and rescue experiments using inhibitor-resistant kinases collectively refute the idea that p38 function is required for dorsal-ventral axis formation and morphogenesis of the sea urchin embryo.

DISCUSSION

A re-evaluation of the role of p38 signalling in dorsal-ventral axis specification

The role of p38 in dorsal-ventral axis formation in the sea urchin was originally discovered on the basis of the inhibitory effect of

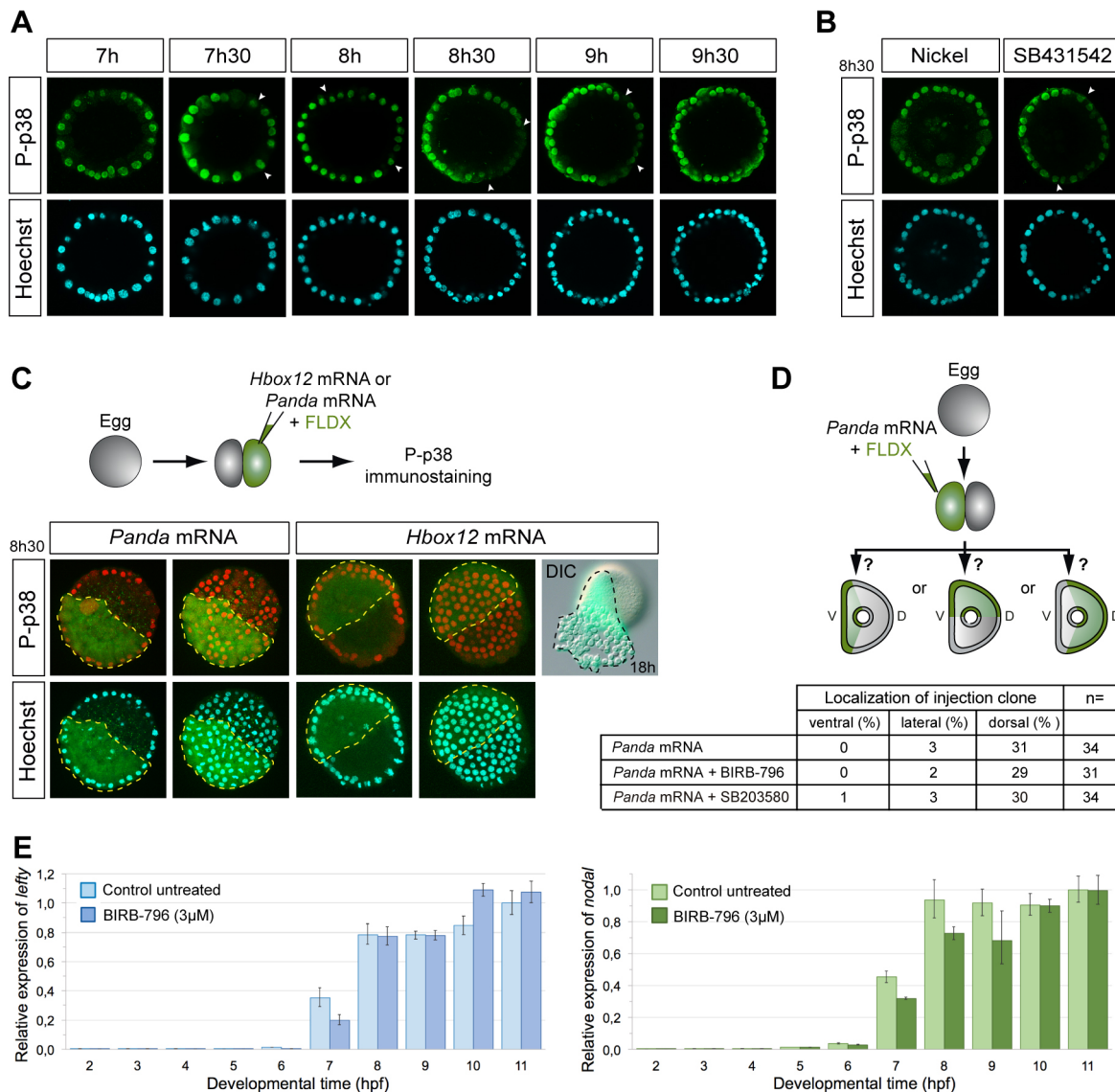


Fig. 7. Transient asymmetric phospho-p38 (P-p38) nuclearization occurs after initiation of *nodal* expression. (A) Time course of P-p38 and Hoechst staining. The clearance of nuclear P-p38 staining is indicated by arrowheads. (B) P-p38 and Hoechst staining after nickel or SB431542 treatments. (C) P-p38 immunostaining, Hoechst staining and morphology of embryos after overexpression of the indicated mRNAs into one blastomere at the two-cell stage (injected cell highlighted with a broken line). Two projections corresponding to the surface or middle confocal sections of the same embryo are shown. Overexpression of *hbox12* causes a massive epithelial-mesenchymal transition that is consistent with this gene being a regulator of PMC fate in the same way as *pmar1* and *micro1*. (A-C) Images are internal projections of around 10 sections from a confocal z-series. (D) Axis orientation assay. Inhibition of p38 activity by the SB203580 or BIRB inhibitors at 3 µM does not affect the ability of *panda* mRNA to orient the dorsal-ventral axis. (E) QPCR analysis of *nodal* and *lefty* expression. Data are mean±s.e.m.

SB203580 on *nodal* expression (Bradham and McClay, 2006). This finding has deeply influenced the field of research on dorsal-ventral axis formation and Nodal signalling during the past 10 years, as it provided a potential link between the spatial regulation of *nodal* and redox gradients present in the early embryo (Coffman and Denegre, 2007). As a consequence, p38 has been included as a key spatial input in all the current models describing the early steps of dorsal-ventral axis formation in the sea urchin embryo. However, despite intense efforts to clarify the relation between the mitochondria, redox gradients, p38 signalling and the transcriptional machinery responsible for initiating *nodal* expression, these links have remained largely obscure (Coffman et al., 2009; Coffman and Denegre, 2007). Furthermore, although bZIP transcription factors are known to mediate the transcriptional effects of p38 (Cuadrado and

Nebreda, 2010), no p38-regulated bZIP transcription factor acting upstream of *nodal* has yet been identified (Nam et al., 2007; Range et al., 2007; Range and Lepage, 2011). Finally, the mechanism responsible for the spatial regulation of p38 has remained elusive.

In this study, we revisited the role of p38 signalling upstream of *nodal* expression using a combination of pharmacological and genetic perturbations. We show that activation or inhibition of p38 signalling does not noticeably affect specification of the dorsal-ventral axis, raising serious doubts as to whether p38 has any function in this process. Furthermore, by analysing the effects of two structurally unrelated families of p38 inhibitors: the pyridinyl-imidazole class represented by SB203580 and SB202190; and the urea-diaryl class, exemplified by BIRB-796, we demonstrate that although both classes of inhibitors efficiently inhibit p38 activity,

only SB203580 and SB202190 but not BIRB-796 interfere with dorsal-ventral axis formation when used at doses twenty to thirty times above that required to inhibit p38 activity effectively. Embryos treated with pyridinyl-imidazole at lower doses (5-10 μM) or with BIRB-796 at doses that eliminated p38 activity develop into normal pluteus larvae with a normal dorsal-ventral axis and a harmoniously patterned skeleton, strongly suggesting that p38 inhibition is responsible neither for the failure of dorsal-ventral axis formation nor for the disruption of skeletogenesis observed in embryos treated with the high doses of SB203580.

Inhibitor-resistant kinases as a means to demonstrate the specificity of kinase inhibitors

A major concern with the use of pharmacological inhibitors is their specificity *in vivo* and the spectrum of 'off targets' that they affect. The crystal structure of p38 bound to SB203580 has been resolved, revealing that the drug becomes inserted into a small hydrophobic pocket deep in the ATP-binding pocket of the kinase, where it interacts with three residues (Thr106, His107 and Leu108) (Tong et al., 1997; Wilson et al., 1997). Threonine 106, also called the gatekeeper residue, plays a particularly important role for the binding of the inhibitor to this hydrophobic pocket; any substitution of this threonine with a residue that has a bigger side chain, such as methionine, reduces the hydrophobic pocket volume, causes the loss of binding of SB203580 and makes the kinase resistant to the inhibitor (Gum et al., 1998). These inhibitor-resistant kinases offer an excellent tool for testing the specificity of kinase inhibitors (Eyers et al., 1998, 1999; Gum et al., 1998; Hall-Jackson et al., 1999; Wilson et al., 1997). We used this strategy to test the specificity of SB203580 in developing sea urchin embryos. As expected, overexpression of a SB203580-resistant p38 kinase restored p38 activity in the presence of SB203580 at high concentrations in an osmotic stress assay. However, this inhibitor-resistant mutant p38 failed to restore *nodal* expression and the dorsal-ventral axis, strongly suggesting that these drugs disrupt dorsal-ventral axis formation indirectly, by 'off target' effects. Furthermore, expression of this inhibitor-resistant p38-MAPK mutant did not restore skeletogenesis, further suggesting that the defects in skeletogenesis observed in SB203580-treated embryos are not due to p38 inhibition. These findings question the strategy used in a recent study (Piacentino et al., 2016) that tried to identify skeletal patterning genes by screening for genes regulated in a similar manner after treatment with NiCl_2 or SB203580, as the two treatments have diametrically opposed effects on *nodal* expression and also because SB203580 strongly disrupts PMC specification and delamination by blocking ERK signalling.

The Nodal receptor Alk4/5/7 is inhibited by pyridinyl-imidazole inhibitors of p38

The specificity of pyridinyl-imidazole class of p38 inhibitors has been questioned in several studies (Bain et al., 2007). In particular, the TGF β receptor Alk5 has been identified as a target of SB203580 inhibition (Laping et al., 2002). The mammalian TGF β receptor Alk5, the type I Activin/Nodal receptors Alk4 and Alk7, and the single sea urchin Nodal receptor Alk4/5/7 all have a serine at the position equivalent to that of Thr106 in p38-MAPK, strongly suggesting that these receptor kinases are also inhibited by SB203580. Indeed, several studies have already warned against the danger of using only pyridinyl-imidazole inhibitors of p38 when evaluating the role of this MAPK in TGF β receptor signalling (Eyers et al., 1998; Fu et al., 2003; Inman et al., 2002; Laping et al., 2002). We confirmed that, in the sea urchin, SB203580 blocks the

activity of the sea urchin Nodal receptor Alk4/5/7 when used at high concentrations. We showed that pre-treatment of embryos with SB203580 at 30 μM eliminated the ability of exogenous Nodal protein, of a constitutively active Nodal receptor or of nickel treatment to induce Nodal target genes. Strikingly, we showed that expression of a modified form of Alk4/5/7 or of ACVRII mutated on a single position equivalent to that of Thr106 on human p38, not only rendered these receptors resistant to the ATP-binding site blocker SB431542 but it also rescued *nodal* expression in embryos that developed in the presence of SB203580 at high doses. Therefore, although it is widely believed that p38 acts upstream of *nodal* expression in the sea urchin, our results show that this conclusion, which was based on the use of high concentrations of pharmacological inhibitors of low specificity, is not correct.

Because our study was performed in *Paracentrotus lividus* whereas the study of Bradham and McClay was performed in *Lytechinus variegatus*, it could be argued that the different results observed in the two studies may reflect species-specific differences. Although such differences cannot be ruled out, we think that it is extremely unlikely that the requirement of p38 in axis specification and skeletogenesis differs in the two species for several reasons. First, the Nodal receptors Alk4/5/7 and ACVRII of *Lytechinus variegatus* both have a serine in the gatekeeper position within the ATP-binding pocket and therefore are predicted to be inhibited by elevated concentrations of SB203580, exactly like their *Paracentrotus* counterparts. Second, we have shown that the p38 inhibitor BIRB-796 potently inhibits p38 activity in *Paracentrotus* without significantly perturbing dorsal-ventral axis formation and morphogenesis, even when used at doses 30 times higher than the dose required to block p38 activity. As it is very unlikely that the three-dimensional structure of p38 from *Lytechinus* differs significantly from that of *Paracentrotus*, we predict that BIRB-796 will also block p38 activity without perturbing morphogenesis in *Lytechinus*. Finally, we have shown that a mutant p38 resistant to SB203580 but capable of activating its downstream targets does not rescue *nodal* expression in the presence of the inhibitor. Because it is unlikely that the downstream effectors of p38 are different in *Lytechinus*, we predict that a mutant p38 resistant to SB203580 will not rescue dorsal-ventral axis formation in this species either.

Why is p38 activation spatially regulated?

Bradham and McClay reported that nuclear p38 is spatially regulated during development, with p38 being first activated in most cells of the blastula stage embryo then cleared from the dorsal side before hatching. In addition, a recent study by Cavalieri and Spinelli using an overexpressed p38-GFP reporter proposed that the homeobox protein Hbox12/Pmar1/Micro1 acts as a repressor of *nodal* expression by repressing the 'activity' of p38 in the presumptive dorsal ectoderm. We have confirmed that p38 activation is spatially regulated during blastula stages. However, our data do not support the hypothesis of Cavalieri and Spinelli on the putative link between Hbox12/Pmar1/Micro1, p38 and *nodal* expression (Cavalieri and Spinelli, 2014; Haillot et al., 2015). p38 is dispensable for *nodal* expression and dorsal-ventral axis formation and Hbox12 does not regulate p38 activation.

The rather late clearance of nuclear p38 is consistent with our finding that p38 is not involved in the initiation of *nodal* expression. However, the dorsal-ventral gradient of nuclear p38 observed as development proceeds suggests that p38 activation may itself be caused by Nodal signalling. Consistent with this idea, a plethora of studies have documented that Activin, Nodal and TGF β signalling induce p38 signalling (Clements et al., 2011; Cocolakis et al., 2001;

Hanafusa et al., 1999; Ogiwara et al., 2003). However, using immunostaining and western blot analysis, we did not find any evidence for p38 being downstream of Nodal signalling. In particular, that this gradient of p38 activity did not disappear following treatment with SB431542 does not support this hypothesis. Alternatively, the gradient of p38 activation may be a consequence of the redox gradients caused by the asymmetrical distribution of mitochondria present in certain batches of eggs (Coffman et al., 2009). Therefore, although we cannot completely rule out a very minor contribution of p38 in dorsal-ventral axis specification downstream of redox gradient, the activity of p38 is needed neither for initiation or maintenance of *nodal* expression nor for the induction of *nodal* target genes; therefore, it is not required for specification of the dorsal-ventral axis.

MATERIALS AND METHODS

All the experiments described in this study have been repeated two or three times. At least 200 wild-type and 50 injected embryos were analysed for each condition or experiment and only phenotypes observed in more than 90% of the embryos are shown.

Animals

Adult sea urchins (*Paracentrotus lividus*) were collected in Villefranche-sur-Mer, France. Embryos were cultured as described elsewhere at 18°C or at the indicated temperature (Lepage and Gache, 1989, 1990).

Treatments

Treatments with recombinant Nodal protein (R&D, 1 µg/ml), NiCl₂ (0.2–0.3 mM), SB203580 (Calbiochem, 559389), SB202190 (Tocris, 1264), SB431542 (Tocris, 1614, 5 µM) and BIRB-796 (Selleckchem, S1574) were started 30 min post-fertilization or at the indicated stages. Stock solutions were prepared in DMSO at 20 mM (SB203580), 10 mM (SB202190 and SB431542) or 1 mM (BIRB-796). The osmotic shock was performed by raising the concentration of NaCl to 1 M for 30 min at hatching blastula stage. The inhibitors were added 30 min before the osmotic shock.

Western blotting

Protein samples equivalent to 600 embryos per well for controls and treated embryos or to 200 embryos per well for injected embryos were separated by SDS-gel electrophoresis and transferred to PVDF membranes. After blocking in 5% dry milk and incubation with the primary antibodies (Cell Signaling Technology) diluted at 1/1000 in 5% BSA, bound antibodies were revealed by ECL immunodetection and imaged with a Fusion Fx7.

Antibodies used were: anti-phospho-p38MAPK(Thr180-Tyr182) (D3F9, catalogue number 4511); anti-phospho-p38MAPK(Thr180-Tyr182) (catalogue number 9211); anti-phospho-MAPKAPK-2(Thr334) (27B7, catalogue number 3007); anti-MAPKAPK-2(D1E11, catalogue number 12155); anti-phospho-p44/42 MAPK(Erk1/2)(Thr202/Tyr 204) (D13.14.4E, catalogue number 4370); anti-phospho-SAPK/JNK(Thr183/Tyr185) (G9, catalogue number 9255); and anti-β-Actin (catalogue number 4967).

Immunostaining

Embryos were fixed with 4% formaldehyde for 15 min then briefly permeabilized with methanol. Anti-phospho-p38-MAPK (Thr180-Tyr182) was used at 1/50. Anti-phospho-p44/42 MAPK (Erk1/2) (Thr202/Tyr 204) was used at 1/500. Hoechst was used to label the nuclei. P-ERK-stained embryos were imaged with an Axio Imager.M2. P-p38 stained embryos were imaged with a Zeiss LSM780 or a Leica SPE confocal microscope.

In situ hybridization

In situ hybridization was performed using standard methods (Harland, 1991) with DIG-labelled RNA probes and developed with NBT/BCIP reagent. Embryos were imaged with an Axio-Imager-M2 microscope.

Plasmid construction and synthetic mRNAs

The constitutively active version of MKK3/6 (MKK3/6-CA, containing the mutations S207E and T211E in the activation loop) was used at 300 µg/ml.

The dominant-negative version of p38 (kinase-dead mutant K54R from the ATP-binding site) was used at 1000 µg/ml. The p38-MKK3/6 construct was made by fusing the wild-type MKK3/6 to p38 using a linker GSLSQGGGGGIL sequence and injected at 300 µg/ml. The gatekeeper mutations of p38, ACVRII and Alk4/5/7 were made by replacing threonine 105, serine 288 and serine 334, respectively, with the more bulky methionine residue. Wild-type p38 and p38T105M were injected at 500 µg/ml. Wild-type Alk4/5/7 was injected at 800 µg/ml and Alk4/5/7 S334M at 500 µg/ml. The wild-type ACVRII and ACVRII S288M were used at 300 µg/ml. At levels higher than these concentrations, MKK3-CA, MKK3-p38 and p38 were toxic and induced apoptosis. All these constructs were made in the pCS2 vector and *in vitro* transcribed using the mMACHINE mMACHINE kit from Ambion. GenBank accession numbers are: p38, KY783932; MKK3/6, KY783933; ACVRII, KY783772; and MAPKAPK, KY783771.

QPCR

QPCR was performed as described previously (Range et al., 2007) on a StepOne instrument. *cyclin-T* was used as a reference gene (Wei et al., 2006). RNA was extracted using Trizol and treated with DNaseI. cDNA synthesis was performed using a mixture of random and anchored oligo-dT20 primers.

Oligonucleotides used were: *nodal*-fwd, 5'-TTCTAAACGGGAGTGC-AAGG; *nodal*-rev, 5'-CTCGGAGTTCAGCAAGATGG; *cyclinT*-fwd, 5'-ACATGATGCCAACAGGTTCC; *cyclinT*-rev, 5'-CAGATGCATCAA-TGGTGGATAA; *lefty*-fwd, 5'-CGGCCCATGCCACAAC; and *lefty*-rev, 5'-CCAAAGAATGGGAGCCTGAA.

Acknowledgements

We thank Benoit Dérjard, Sébastien Huaud, Laurent Turchi and Laurent Gagnoux for providing us with reagents and protocols, and for stimulating discussions on MAPK biochemistry. We thank Salsabiel El Nagar for advice regarding QPCR and Benoit Dérjard for careful reading of the manuscript.

Competing interests

The authors declare no competing or financial interests.

Author contributions

Conceptualization: M.D.M., E.H., T.L.; Methodology: M.D.M., M.Q., E.H., F.J., A.C., T.L.; Validation: M.D.M., M.Q., E.H., T.L.; Formal analysis: M.D.M.; Investigation: M.Q., E.H., T.L., M.D.M. Data curation: M.D.M.; Writing - original draft: M.D.M., T.L.; Writing - review & editing: M.D.M., T.L.; Supervision: T.L.; Project administration: T.L.; Funding acquisition: T.L.

Funding

This work was supported by grants from the Centre National de la Recherche Scientifique, the University of Nice Sophia-Antipolis, the Association pour la Recherche sur le Cancer (ARC) (SF120121205586) and the Agence Nationale de la Recherche (ANR) (grant entitled 'Echinodal', 14-CE11-0006-01). M.D.M. was supported by a European Molecular Biology Organization long-term fellowship and by an ARC postdoctoral fellowship. M.Q. and E.H. were supported by a 4th year doctoral fellowship from the ARC.

Supplementary information

Supplementary information available online at <http://dev.biologists.org/lookup/doi/10.1242/dev.152330.supplemental>

References

- Bain, J., Plater, L., Elliott, M., Shpiro, N., Hastie, C. J., McLauchlan, H., Klevernic, I., Arthur, J. S. C., Alessi, D. R. and Cohen, P. (2007). The selectivity of protein kinase inhibitors: a further update. *Biochem. J.* **408**, 297-315.
- Bradham, C. A. and McClay, D. R. (2006). p38 MAPK is essential for secondary axis specification and patterning in sea urchin embryos. *Development* **133**, 21-32.
- Bradham, C. A., Oikonomou, C., Kühn, A., Core, A. B., Modell, J. W., McClay, D. R. and Poustka, A. J. (2009). Chordin is required for neural but not axial development in sea urchin embryos. *Dev. Biol.* **328**, 221-233.
- Cavaliere, V. and Spinelli, G. (2014). Early asymmetric cues triggering the dorsal/ventral gene regulatory network of the sea urchin embryo. *Elife* **3**, e04664.
- Clements, M., Pernaute, B., Vella, F. and Rodriguez, T. A. (2011). Crosstalk between Nodal/activin and MAPK p38 signaling is essential for anterior-posterior axis specification. *Curr. Biol.* **21**, 1289-1295.

- Cocolakis, E., Lemay, S., Ali, S. and Lebrun, J. J.** (2001). The p38 MAPK pathway is required for cell growth inhibition of human breast cancer cells in response to activin. *J. Biol. Chem.* **276**, 18430-18436.
- Coffman, J. A. and Denegre, J. M.** (2007). Mitochondria, redox signaling and axis specification in metazoan embryos. *Dev. Biol.* **308**, 266-280.
- Coffman, J. A., Coluccio, A., Planchart, A. and Robertson, A. J.** (2009). Oral-aboral axis specification in the sea urchin embryo III. Role of mitochondrial redox signaling via H₂O₂. *Dev. Biol.* **330**, 123-130.
- Cuadrado, A. and Nebreda, A. R.** (2010). Mechanisms and functions of p38 MAPK signalling. *Biochem. J.* **429**, 403-417.
- Duboc, V., Röttinger, E., Besnardeau, L. and Lepage, T.** (2004). Nodal and BMP2/4 signaling organizes the oral-aboral axis of the sea urchin embryo. *Dev. Cell* **6**, 397-410.
- Duloquin, L., Lhomond, G. and Gache, C.** (2007). Localized VEGF signaling from ectoderm to mesenchyme cells controls morphogenesis of the sea urchin embryo skeleton. *Development* **134**, 2293-2302.
- Eyers, P. A., Craxton, M., Morrice, N., Cohen, P. and Goedert, M.** (1998). Conversion of SB 203580-insensitive MAP kinase family members to drug-sensitive forms by a single amino-acid substitution. *Chem. Biol.* **5**, 321-328.
- Eyers, P. A., van den IJssel, P., Quinlan, R. A., Goedert, M. and Cohen, P.** (1999). Use of a drug-resistant mutant of stress-activated protein kinase 2a/p38 to validate the in vivo specificity of SB 203580. *FEBS Lett.* **451**, 191-196.
- Fernandez-Serra, M., Consales, C., Livigni, A. and Arnone, M. I.** (2004). Role of the ERK-mediated signaling pathway in mesenchyme formation and differentiation in the sea urchin embryo. *Dev. Biol.* **268**, 384-402.
- Fu, Y., O'Connor, L. M., Shepherd, T. G. and Nachtigal, M. W.** (2003). The p38 MAPK inhibitor, PD169316, inhibits transforming growth factor beta-induced Smad signaling in human ovarian cancer cells. *Biochem. Biophys. Res. Commun.* **310**, 391-397.
- Gum, R. J., McLaughlin, M. M., Kumar, S., Wang, Z., Bower, M. J., Lee, J. C., Adams, J. L., Livi, G. P., Goldsmith, E. J. and Young, P. R.** (1998). Acquisition of sensitivity of stress-activated protein kinases to the p38 inhibitor, SB 203580, by alteration of one or more amino acids within the ATP binding pocket. *J. Biol. Chem.* **273**, 15605-15610.
- Haillot, E., Molina, M. D., Lapraz, F. and Lepage, T.** (2015). The maternal maverick/GDF15-like TGF-beta ligand panda directs dorsal-ventral axis formation by restricting nodal expression in the sea urchin embryo. *PLoS Biol.* **13**, e1002247.
- Hall-Jackson, C. A., Goedert, M., Hedge, P. and Cohen, P.** (1999). Effect of SB 203580 on the activity of c-Raf in vitro and in vivo. *Oncogene* **18**, 2047-2054.
- Han, J., Lee, J. D., Bibbs, L. and Ulevitch, R. J.** (1994). A MAP kinase targeted by endotoxin and hyperosmolarity in mammalian cells. *Science* **265**, 808-811.
- Hanafusa, H., Ninomiya-Tsuji, J., Masuyama, N., Nishita, M., Fujisawa, J., Shibuya, H., Matsumoto, K. and Nishida, E.** (1999). Involvement of the p38 mitogen-activated protein kinase pathway in transforming growth factor-beta-induced gene expression. *J. Biol. Chem.* **274**, 27161-27167.
- Harland, R. M.** (1991). In situ hybridization: an improved whole-mount method for *Xenopus* embryos. *Methods Cell Biol.* **36**, 685-695.
- Ho, D. M., Chan, J., Bayliss, P. and Whitman, M.** (2006). Inhibitor-resistant type I receptors reveal specific requirements for TGF-beta signaling in vivo. *Dev. Biol.* **295**, 730-742.
- Inman, G. J., Nicolas, F. J., Callahan, J. F., Harling, J. D., Gaster, L. M., Reith, A. D., Laping, N. J. and Hill, C. S.** (2002). SB-431542 is a potent and specific inhibitor of transforming growth factor-beta superfamily type I activin receptor-like kinase (ALK) receptors ALK4, ALK5, and ALK7. *Mol. Pharmacol.* **62**, 65-74.
- Kitamura, K., Nishimura, Y., Kubotera, N., Higuchi, Y. and Yamaguchi, M.** (2002). Transient activation of the micro1 homeobox gene family in the sea urchin (*Hemicentrotus pulcherrimus*) micromere. *Dev. Genes Evol.* **212**, 1-10.
- Kuma, Y., Sabio, G., Bain, J., Shpiro, N., Márquez, R. and Cuenda, A.** (2005). BIRB796 inhibits all p38 MAPK isoforms in vitro and in vivo. *J. Biol. Chem.* **280**, 19472-19479.
- Laping, N. J., Grygielko, E., Mathur, A., Butter, S., Bomberger, J., Tweed, C., Martin, W., Fornwald, J., Lehr, R., Harling, J. et al.** (2002). Inhibition of transforming growth factor (TGF)-beta1-induced extracellular matrix with a novel inhibitor of the TGF-beta type I receptor kinase activity: SB-431542. *Mol. Pharmacol.* **62**, 58-64.
- Lapraz, F., Röttinger, E., Duboc, V., Range, R., Duloquin, L., Walton, K., Wu, S.-Y., Bradham, C., Loza, M. A., Hibino, T. et al.** (2006). RTK and TGF-beta signaling pathways genes in the sea urchin genome. *Dev. Biol.* **300**, 132-152.
- Lapraz, F., Besnardeau, L. and Lepage, T.** (2009). Patterning of the dorsal-ventral axis in echinoderms: insights into the evolution of the BMP-Chordin signaling Network. *PLoS Biol.* **7**, 1-25.
- Lee, J. C., Laydon, J. T., McDonnell, P. C., Gallagher, T. F., Kumar, S., Green, D., McNulty, D., Blumenthal, M. J., Keys, J. R., Landvatter, S. W. et al.** (1994). A protein kinase involved in the regulation of inflammatory cytokine biosynthesis. *Nature* **372**, 739-746.
- Lepage, T. and Gache, C.** (1989). Purification and characterization of the sea urchin embryo hatching enzyme. *J. Biol. Chem.* **264**, 4787-4793.
- Lepage, T. and Gache, C.** (1990). Early expression of a collagenase-like hatching enzyme gene in the sea urchin embryo. *EMBO J.* **9**, 3003-3012.
- McClay, D. R., Peterson, R. E., Range, R. C., Winter-Vann, A. M. and Ferkowicz, M. J.** (2000). A micromere induction signal is activated by beta-catenin and acts through notch to initiate specification of secondary mesenchyme cells in the sea urchin embryo. *Development* **127**, 5113-5122.
- Molina, M. D., de Croze, N., Haillot, E. and Lepage, T.** (2013). Nodal: master and commander of the dorsal-ventral and left-right axes in the sea urchin embryo. *Curr. Opin. Genet. Dev.* **23**, 445-453.
- Nam, J., Su, Y.-H., Lee, P. Y., Robertson, A. J., Coffman, J. A. and Davidson, E. H.** (2007). Cis-regulatory control of the nodal gene, initiator of the sea urchin oral ectoderm gene network. *Dev. Biol.* **306**, 860-869.
- Nishimura, Y., Sato, T., Morita, Y., Yamazaki, A., Akasaka, K. and Yamaguchi, M.** (2004). Structure, regulation, and function of micro1 in the sea urchin *Hemicentrotus pulcherrimus*. *Dev. Genes Evol.* **214**, 525-536.
- Ogihara, T., Watada, H., Kanno, R., Ikeda, F., Nomiya, T., Tanaka, Y., Nakao, A., German, M. S., Kojima, I. and Kawamori, R.** (2003). p38 MAPK is involved in activin A- and hepatocyte growth factor-mediated expression of pro-endocrine gene neurogenin 3 in AR42J-B13 cells. *J. Biol. Chem.* **278**, 21693-21700.
- Oliveri, P., Davidson, E. H. and McClay, D. R.** (2003). Activation of pmar1 controls specification of micromeres in the sea urchin embryo. *Dev. Biol.* **258**, 32-43.
- Oliveri, P., Walton, K. D., Davidson, E. H. and McClay, D. R.** (2006). Repression of mesodermal fate by foxa, a key endoderm regulator of the sea urchin embryo. *Development* **133**, 4173-4181.
- Pargellis, C., Tong, L., Churchill, L., Cirillo, P. F., Gilmore, T., Graham, A. G., Grob, P. M., Hickey, E. R., Moss, N., Pav, S. et al.** (2002). Inhibition of p38 MAP kinase by utilizing a novel allosteric binding site. *Nat. Struct. Biol.* **9**, 268-272.
- Piacentino, M. L., Zuch, D. T., Fishman, J., Rose, S., Speranza, E. E., Li, C., Yu, J., Chung, O., Ramachandran, J., Ferrell, P. et al.** (2016). RNA-Seq identifies SPGs as a ventral skeletal patterning cue in sea urchins. *Development* **143**, 703-714.
- Raingaud, J., Gupta, S., Rogers, J. S., Dickens, M., Han, J., Ulevitch, R. J. and Davis, R. J.** (1995). Pro-inflammatory cytokines and environmental stress cause p38 mitogen-activated protein kinase activation by dual phosphorylation on tyrosine and threonine. *J. Biol. Chem.* **270**, 7420-7426.
- Range, R. and Lepage, T.** (2011). Maternal Oct1/2 is required for Nodal and Vg1/Univin expression during dorsal-ventral axis specification in the sea urchin embryo. *Dev. Biol.* **357**, 440-449.
- Range, R., Lapraz, F., Quirin, M., Marro, S., Besnardeau, L. and Lepage, T.** (2007). Cis-regulatory analysis of nodal and maternal control of dorsal-ventral axis formation by Univin, a TGF-beta related to Vg1. *Development* **134**, 3649-3664.
- Ransick, A. and Davidson, E. H.** (2006). cis-regulatory processing of Notch signaling input to the sea urchin glial cells missing gene during mesoderm specification. *Dev. Biol.* **297**, 587-602.
- Röttinger, E., Besnardeau, L. and Lepage, T.** (2004). A Raf/MEK/ERK signaling pathway is required for development of the sea urchin embryo micromere lineage through phosphorylation of the transcription factor Ets. *Development* **131**, 1075-1087.
- Rouse, J., Cohen, P., Trigon, S., Morange, M., Alonso-Llamazares, A., Zamanillo, D., Hunt, T. and Nebreda, A. R.** (1994). A novel kinase cascade triggered by stress and heat shock that stimulates MAPKAP kinase-2 and phosphorylation of the small heat shock proteins. *Cell* **78**, 1027-1037.
- Saudemont, A., Haillot, E., Mekpoh, F., Bessodes, N., Quirin, M., Lapraz, F., Duboc, V., Röttinger, E., Range, R., Oisel, A. et al.** (2010). Ancestral regulatory circuits governing ectoderm patterning downstream of Nodal and BMP2/4 revealed by gene regulatory network analysis in an echinoderm. *PLoS Genet.* **6**, e1001259.
- Sweet, H. C., Gehring, M. and Ettensohn, C. A.** (2002). LvDelta is a mesoderm-inducing signal in the sea urchin embryo and can endow blastomeres with organizer-like properties. *Development* **129**, 1945-1955.
- Tong, L., Pav, S., White, D. M., Rogers, S., Crane, K. M., Cywin, C. L., Brown, M. L. and Pargellis, C. A.** (1997). A highly specific inhibitor of human p38 MAP kinase binds in the ATP pocket. *Nat. Struct. Biol.* **4**, 311-316.
- Tu, Q., Brown, C. T., Davidson, E. H. and Oliveri, P.** (2006). Sea urchin Forkhead gene family: Phylogeny and embryonic expression. *Dev. Biol.* **300**, 49-62.
- Wei, Z., Angerer, R. C. and Angerer, L. M.** (2006). A database of mRNA expression patterns for the sea urchin embryo. *Dev. Biol.* **300**, 476-484.
- Wikramanayake, A. H., Huang, L. and Klein, W. H.** (1998). beta-Catenin is essential for patterning the maternally specified animal-vegetal axis in the sea urchin embryo. *Proc. Natl. Acad. Sci. USA* **95**, 9343-9348.
- Wilson, K. P., McCaffrey, P. G., Hsiao, K., Pazhanisamy, S., Galullo, V., Bemis, G. W., Fitzgibbon, M. J., Caron, P. R., Murcko, M. A. and Su, M. S. S.** (1997). The structural basis for the specificity of pyridinylimidazole inhibitors of p38 MAP kinase. *Chem. Biol.* **4**, 423-431.
- Yaguchi, S., Yaguchi, J. and Burke, R. D.** (2006). Specification of ectoderm restricts the size of the animal plate and patterns neurogenesis in sea urchin embryos. *Development* **133**, 2337-2346.